A R C H I V E S O F M E T A L L U R G Y A N D M A T E R I A L S
Volume 55 2010 Issue 1

M. NABIAŁEK*, J. ZBROSZCZYK*, W. CIURZYŃSKA*, J. OLSZEWSKI*, S. LESZ**, P. BRĄGIEL***, J. GONDRO*, K. SOBCZYK*, A. ŁUKIEWSKA*, J. ŚWIERCZEK*, P. PIETRUSIEWICZ*

MICROSTRUCTURE, SOME MAGNETIC AND MECHANICAL PROPERTIES OF AMORPHOUS $Fe_{60}Co_{10}Zr_{2.5}Hf_{2.5}W_2Y_2B_{21}$ PLATES

MIKROSTRUKTURA, STABILNOŚĆ TERMICZNA I MAGNETYCZNE WŁAŚCIWOŚCI MASYWNEGO STOPU AMORFICZNEGO $Fe_{61}Co_{10}Zr_{2,5}W_2Hf_{2,5}Y_2B_{20}$

In this paper we present the results of microstructure, thermal stability and magnetic properties studies for the bulk amorphous $Fe_{61}Co_{10}Zr_{2.5}Hf_{2.5}W_2Y_2B_{20}$ alloy in the form of plates 0.5 mm in thickness prepared at different cooling rates (in a mould cooled with water and without cooling with water). We have stated that the investigated alloy exhibits good glass-forming ability. The amorphous plates obtained at larger cooling rate show a slightly higher crystallization temperature. SEM micrographs on the fraction surface of the plates reveal parallel and curved bands. The chemical composition on the fraction surface determined from EDS studies is close to the nominal composition of the alloy. The amorphous plates prepared at larger cooling rate exhibit better soft magnetic properties.

Keywords: bulk amorphous alloy, Mössbauer spectroscopy, thermal stability, X-ray spectrometer (EDS), core losses

W pracy przedstawiono wyniki badań mikrostruktury, stabilności termicznej i właściwości magnetycznych masywnego stopu amorficznego $Fe_{61}Co_{10}Zr_{2.5}Hf_{2.5}W_2Y_2B_{20}$ w postaci płytek o grubości 0,5 mm. Próbki przygotowano techniką szybkiego chłodzenia (w formie chłodzonej wodą i bez chłodzenia). Otrzymany stop wykazywał dobrą zdolność do zeszklenia. Amorficzne płytki wytworzone z większą szybkością chłodzenia cechowały się nieco wyższą temperaturą krystalizacji. Na obrazach struktury przełomów płytek uzyskanych za pomocą mikroskopu skaningowego widoczne są liniowe równoległe i zakrzywione pasma. Analizę chemiczną składu stopu wykonano metodą EDS, skład otrzymanych próbek był zgodny ze składem nominalnym. Amorficzne płytki wykonane z dużą szybkością chłodzenia wykazywały lepsze miękkie właściwości magnetyczne.

1. Introduction

It is well known that Fe-Co based amorphous alloys exhibit better soft magnetic properties than silicon steel [1, 2] and they are usually prepared in the form of thin ribbons with thickness of about 20 μm. However, the application of these materials in electrical industry is limited by thinness of gauge, brittleness after a heat treatment and stress sensitivity. Contrary to classical crystalline Fe-Si sheets it is impossible to make magnetic cores from the amorphous classical alloys with high mass packing density because of air gaps between the large number of thin ribbons. A suction casting method [3, 4] enables to obtain amorphous alloys in the form of rods, tubes, plates and cores with a very complicated shape. On account of excellent soft magnetic and mechanical properties, Fe-Co based bulk amorphous alloys are interesting for both scientific research and technological applications.

In this paper we present results of microstructure, its thermal stability, magnetic and mechanical properties studies of the amorphous $Fe_{61}Co_{10}Zr_{2.5}Hf_{2.5}W_2Y_2B_{20}$ plates.

2. Experimental procedure

The amorphous $Fe_{61}Co_{10}Zr_{2.5}Hf_{2.5}W_2Y_2B_{21}$ plates were prepared from ingots obtained by arc-melting in an argon atmosphere. The plates with 0.5 mm thickness were produced by rapid solidification of the molten material in a copper mould cooled with water or without cooling with water. The microstructure was studied

* INSTITUTE OF PHYSICS, CZĘSTOCHOWA UNIVERSITY OF TECHNOLOGY, 42-200 CZĘSTOCHOWA, 19 ARMII KRAJOWEJ AV., POLAND
** INSTITUTE OF ENGINEERING MATERIALS AND BIOMATERIALS, SILESIAN TECHNICAL UNIVERSITY, 18A KONARSKIEGO STR., 44-100 GLIWICE, POLAND
*** INSTITUTE OF PHYSICS, JAN DLUGOSZ UNIVERSITY, 42-200 CZĘSTOCHOWA, 13/15 ARMII KRAJOWEJ AV., POLAND

for powdered samples using X-ray diffractometer and Mössbauer spectrometer. Mössbauer spectra were fitted with NORMOS package to obtain distribution of magnetic hyperfine field [5]. Thermal stability of the alloys was investigated by differential scanning calorymetry (DSC). The fracture morphology of the plates and elements distribution in them has been studied using a scanning electron microscope and an X-ray spectrometer (EDS), respectively. The saturation magnetic polarization and coercivity were determined from magnetization curves and hysteresis loops measured by a vibrating sample magnetometer (VSM). Core losses of the samples were studied by the transformer method using a completely automated set-up.

3. Results and discussion

X-ray diffraction patterns of the powdered as-quenched $Fe_{61}Co_{10}Zr_{2.5}Hf_{2.5}W_2Y_2B_{20}$ plates at room temperature are displayed in Fig 1. No sharp peaks are seen in diffraction patterns of both plates which indicates that investigated alloys in the as-quenched state are fully amorphous. The amorphicity of the samples was also confirmed by Mössbauer studies. The transmission Mössbauer spectra obtained at room temperature of the investigated $Fe_{61}Co_{10}Zr_{2.5}Hf_{2.5}W_2Y_2B_{20}$ alloys are presented in Fig. 2.

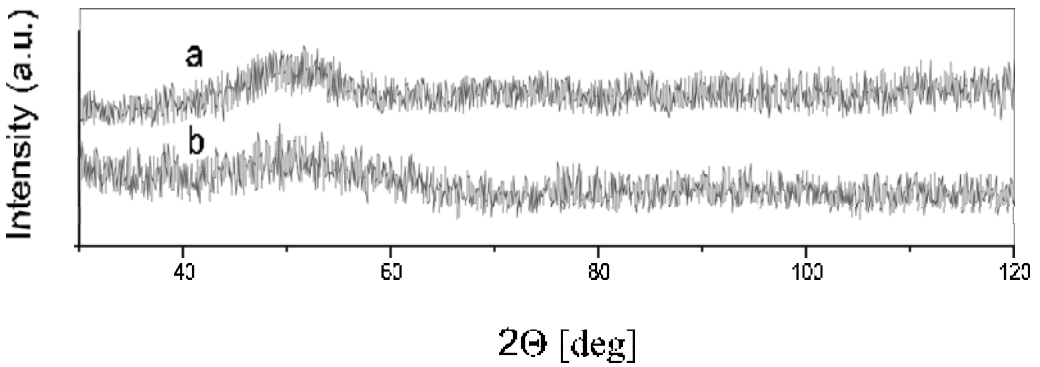

Fig. 1. 1 X-ray diffraction patterns of the as-quenched $Fe_{61}Co_{10}Zr_{2.5}Hf_{2.5}W_2Y_2B_{20}$ plates after powdering: mould cooled with water (a), without cooling with water (b)

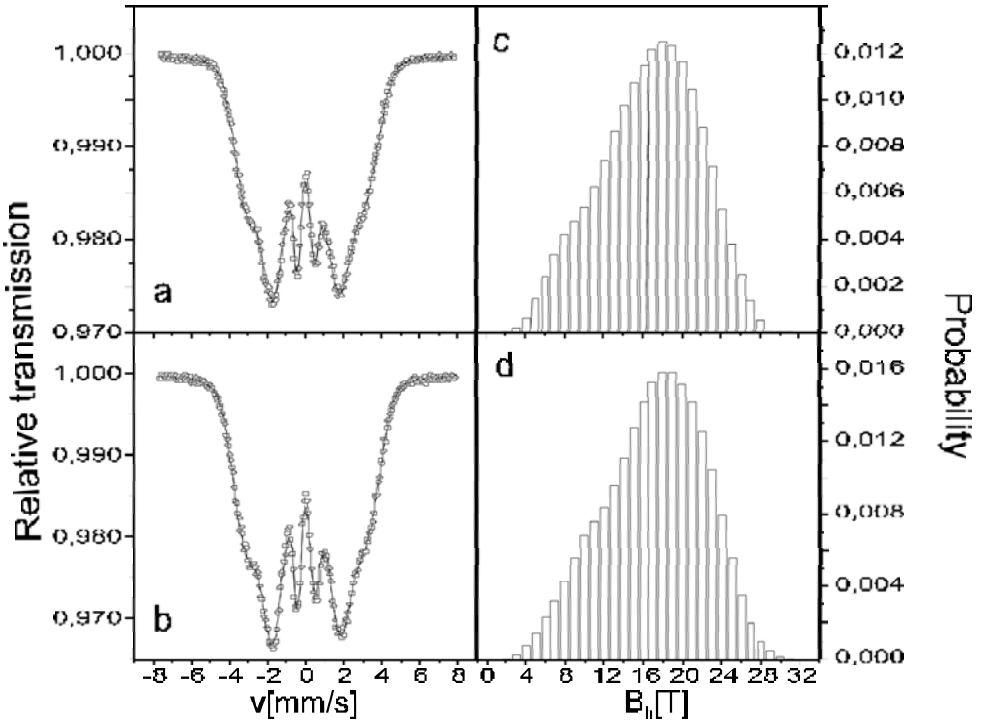

Fig. 2. Transmission Mössbauer spectra (a, b) and corresponding hyperfine field distributions (c, d) of powdered $Fe_{61}Co_{10}Zr_{2.5}Hf_{2.5}W_2Y_2B_{20}$ plates after solidification: mould cooled with water (a, c) and without cooling with water (b, d)

The Möössbauer spectra show a broad but well defined magnetic structure which is characteristic of amorphous materials. From the shape of fitted distributions of hyperfine field induction $P(B_h)$ we may state that the investigated alloys are relatively homogenous because $P(B_h)$ is almost symmetrical (Fig. 2 c, d). However, in these distributions low and high field components may be distinguished. The results of X-ray and Mössbauer spectroscopy studies obtained for this alloy confirm its good glass-forming ability. In Fig 3 DSC curves of the as-quenched plates recorded at the heating rate of 10 K/min are presented. In DSC curves the pronounced peaks at about 870 K associated with crystallization processes are seen. In comparison with the classical amorphous materials the investigated alloy crystallizes at higher temperature [6]. From these results we may state that the investigated plates exhibit good thermal stability of the structure. Parameters determined from the analysis of DSC curves [7, 8] are collected in Table 1. It is evident that the investigated alloy exhibits the higher glass transition temperature (T_g), onset crystallization temperature (T_x) and liquidus temperature (T_l) than the bulk Fe-based amorphous alloys of similar composition [9]. Moreover, the bulk amorphous $Fe_{61}Co_{10}Zr_{2.5}Hf_{2.5}W_2Y_2B_{20}$ alloy shows large values of the temperature interval of the supercooled liquid region before crystallization (ΔT_x), which is equal to 80 K and 78 K for the alloy obtained in the mould cooled with water (sample a) and in the mould without cooling with water (sample b), respectively. It is worth noticing that the parameter ΔT_x is usually equal to about 60 K for other ferromagnetic alloys [9]. The bulk $Fe_{61}Co_{10}Zr_{2.5}Hf_{2.5}W_2Y_2B_{20}$ alloy also exhibits the large value of parameters $\gamma = T_x/(T_g+T_l)$ and $\delta = T_x/(T_l-T_g)$ determining their good glass-forming ability, which are comparable with those described in [10]. From the results presented in this table we may also state that the sample of the bulk $Fe_{61}Co_{10}Zr_{2.5}Hf_{2.5}W_2Y_2B_{20}$ alloy obtained in the mould without cooling with water shows lower onset crystallization temperature. This sample was prepared with the lower cooling rate and structure relaxations occurred during the preparation process. It is well known that the crystalline grains grow from as-quenched and created during annealing nuclei due to irreversible relaxations. This process is thermally activated and occurs at lower temperature than for the sample prepared in the mould cooled with water.

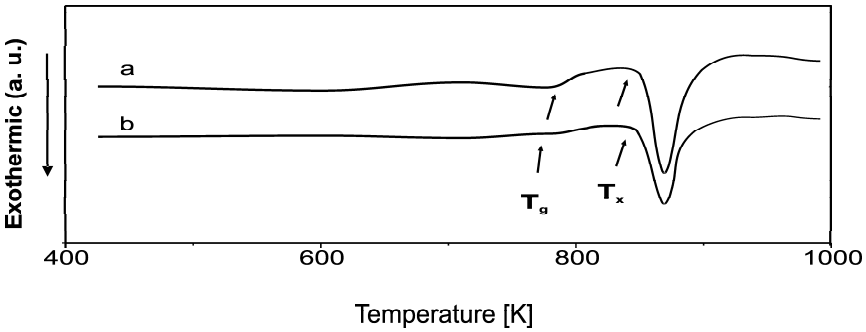

Fig. 3. DSC curves of the amorphous $Fe_{61}Co_{10}Zr_{2.5}Hf_{2.5}W_2Y_2B_{20}$ plates after solidification: mould cooled with water (a), without cooling with water (b)

TABLE 1

Parameters calculated from DSC curves obtained for $Fe_{61}Co_{10}Zr_{2.5}Hf_{2.5}W_2Y_2B_{20}$ plates: mould cooled with water (sample a) and mould without cooling with water (sample b); glass transition temperature (T_g), crystallization onset temperature (T_x), melting temperature (T_m), liquidus temperature (T_l) and the values of several glass forming parameters; $\Delta T_m = T_l - T_m$, $\Delta T_l = T_l - T_x$, the supercooled liquid region (ΔT_x), $\gamma = T_x/(T_g+T_l)$, $\delta = T_x/(T_l-T_g)$, and the reduced glass transition temperature (T_g/T_m)

$Fe_{61}Co_{10}Zr_{2.5}$ $Hf_{2.5}W_2Y_2B_{20}$	T_g [K]	T_x [K]	T_m [K]	T_l [K]	ΔT_m [K]	ΔT_l [K]	ΔT_x [K]	T_{rg} [K]	γ	δ
Sample a	792 ± 1	872 ± 1	1336 ± 1	1462 ± 1	126 ± 2	590 ± 2	80 ± 2	0,593 ± 0,003	0,386 ± 0,002	1,301 ± 0,005
Sample b	788 ± 1	866 ± 1	1332 ± 1	1455 ± 1	123 ± 2	589 ± 2	78 ± 2	0,591 ± 0,003	0,351 ± 0,002	1,298 ± 0,003

SEM fracture morphology of $Fe_{61}Co_{10}Zr_{2.5}Hf_{2.5}W_2Y_2B_{20}$ plates are presented in Fig. 4. The parallel and curved bands [11] are mainly seen in these micrographs (Fig. 4a) confirming full amorphicity of the sample. It is worth noticing that in the micrograph of the fracture surface of the sample prepared with lower cooling rate (Fig. 4b) apart from the parallel and curved bands, the particle - like figures are presented. It indicates that the sample obtained in the mould without cooling is less homogenous than the previous one (Fig. 4a). Using an X-ray spectrometer the element distribution in fraction surface (marked rectangle in Fig. 4) was determined. The dependence of X-ray intensity of analyzed elements on photon energy is shown in Fig. 5.

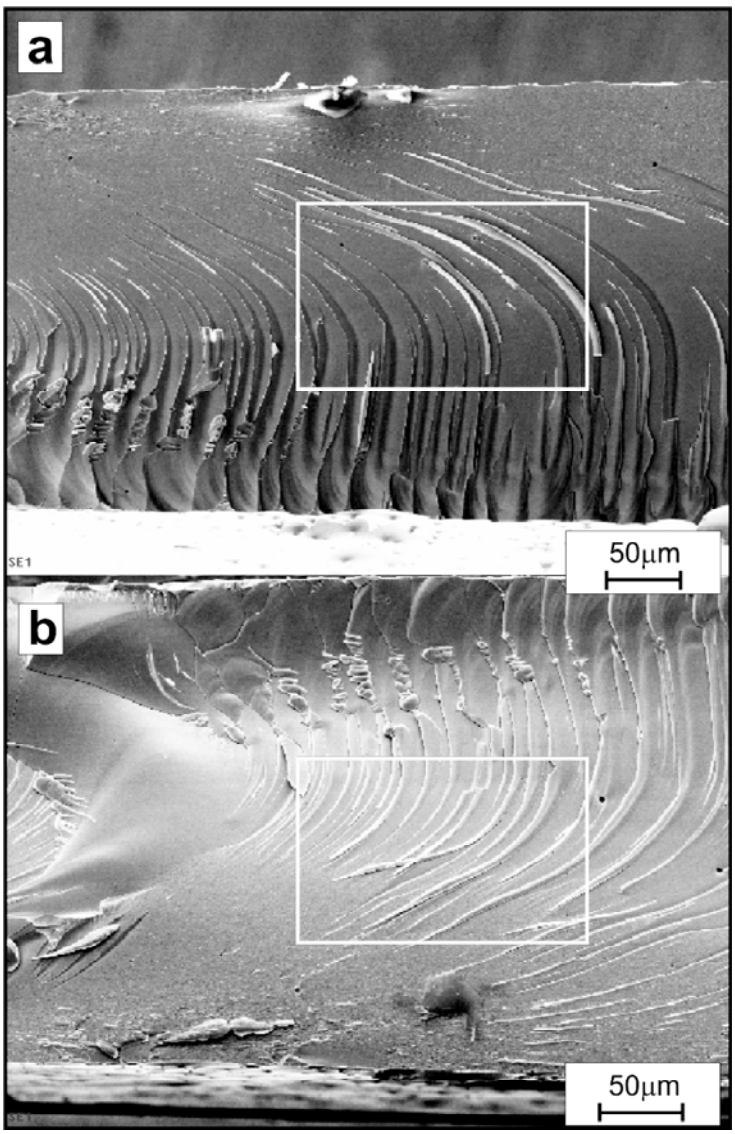

Fig. 4. SEM fracture morphology of the as-quenched $Fe_{61}Co_{10}Zr_{2.5}Hf_{2.5}W_2Y_2B_{20}$ plates: mould cooled with water (a) and mould without cooling with water (b)

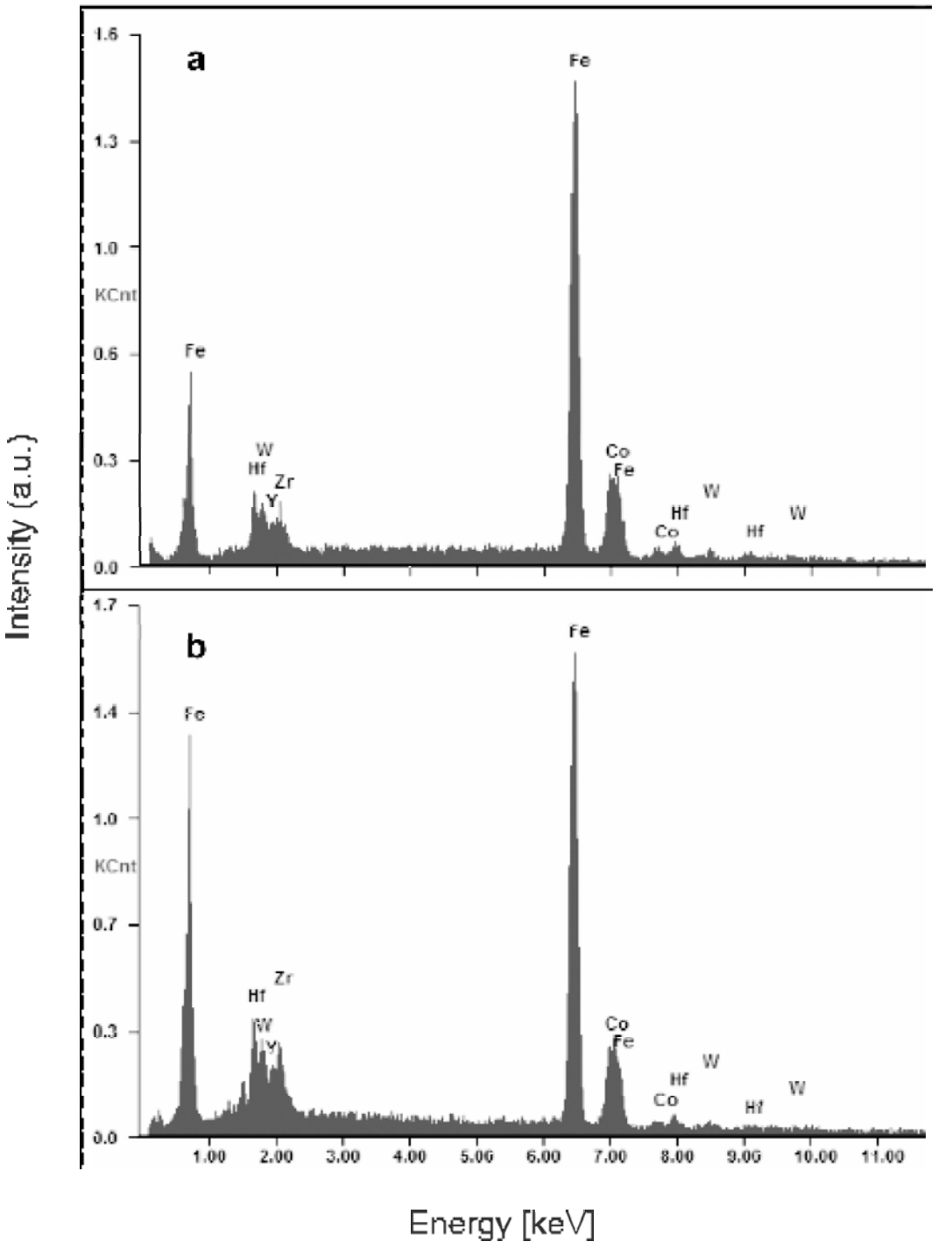

Fig. 5. Intensity of X-ray lines for analyzed elements as a function of photon energy for plates obtained in the mould cooled with water (a) and in the mould without cooling with water (b)

Assuming that the boron atom concentration in the investigated alloy is equal to 20% the other element distribution on the fracture surface (inside marked rectangles in Fig. 4) are evaluated and the obtained results are collected in Table 2. From the results presented in Table 2 we may assume that the element distribution in the fraction surface of plates is close to the nominal composition of the alloy.

TABLE 2

Chemical composition in the fracture surface of $Fe_{61}Co_{10}Zr_{2.5}Hf_{2.5}W_2Y_2B_{20}$ plates after solidification determined by EDS method: mould cooled with water (sample a) and mould without cooling with water (sample b)

	at %	
Element	Sample a	Sample b
Fe	60,704	58,400
Co	10,720	11,224
Zr	1,936	3,296
Hf	2,824	2,944
Y	1,752	2,256
W	2,072	1,880
B	20	20
Sum	100	100

This alloy is a soft ferromagnet and the coercive field determined from hysteresis loops is equal to 70 A/m and 90 A/m for the plate prepared in the mould cooled with water and without cooling with water, respectively. The value of the coercivity is comparable with that observed for classical crystalline Fe-Si alloys and is accompanied by a relatively high magnetic polarization saturation equal to 0.98 T. Preparation conditions of amorphous alloys also influence their magnetic susceptibility. In Fig. 6 the magnetic susceptibility as a function of the magnetizing field amplitude is depicted. It is seen that the plate obtained at the higher cooling rate exhibits larger relative magnetic permeability.

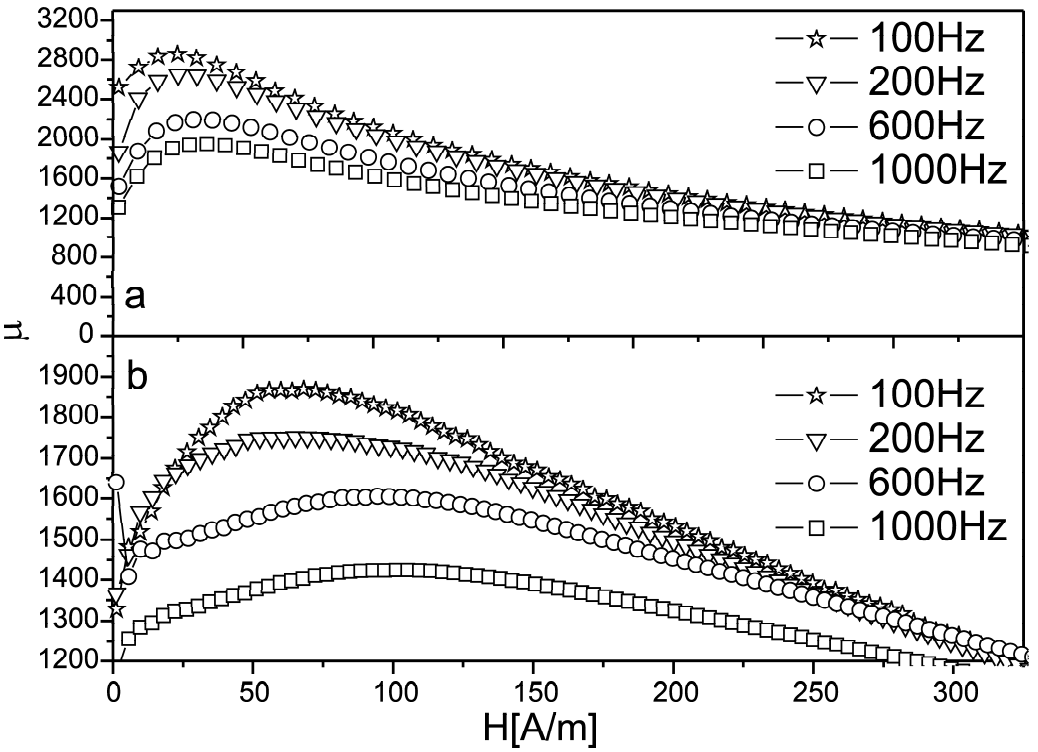

Fig. 6. Dependence of the relative magnetic permeability on the amplitude of magnetizing field for $Fe_{61}Co_{10}Zr_{2.5}Hf_{2.5}W_2Y_2B_{20}$ alloy after solidification: plate prepared in the mould cooled with water (a) and in the mould without cooling with water (b)

Fig. 7 shows the dependence of core losses on maximum induction for the investigated amorphous plates (for three frequencies of the magnetizing field).

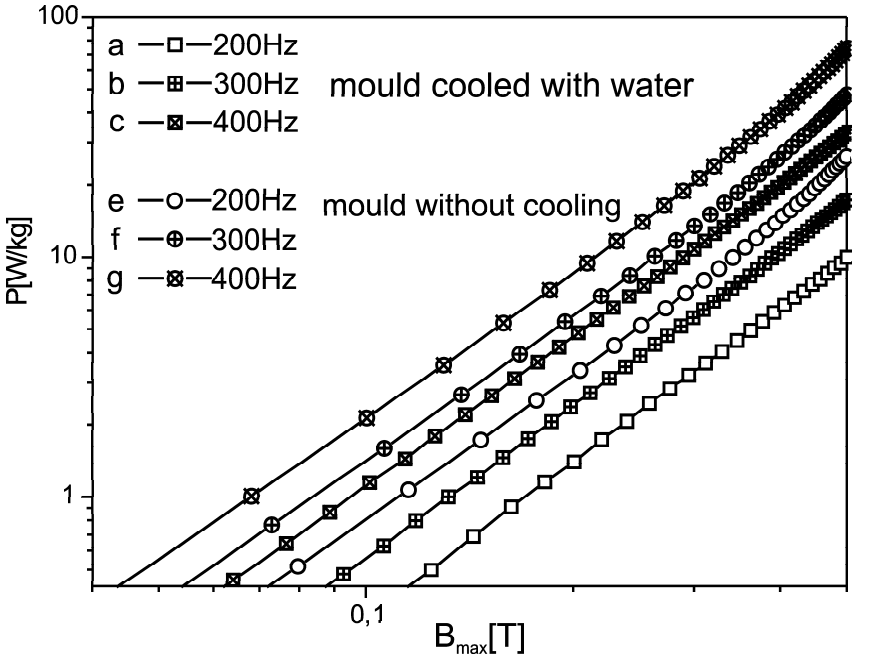

Fig. 7. Core losses as a function of the maximum induction for the as-quenched $Fe_{61}Co_{10}Zr_{2.5}Hf_{2.5}W_2Y_2B_{20}$ alloy: plate prepared in the mould cooled with water (a, b, c), in the mould without cooling with water (d, e, f)

The plate obtained in the mould cooled with water shows lower core losses than that prepared at lower quenching rate.

Summing up, the plate prepared at low quenching rate (in the mould without cooling with water) shows weaker soft magnetic properties which is presumably connected with the decomposition of the amorphous state and creation of domain walls pinning centers.

4. Conclusions

1. The investigated alloy exhibits good glass-forming ability.
2. The sample obtained at lower cooling rate shows lower crystallization onset temperature.
3. The chemical composition of the alloy determined from the results obtained by EDS method is closed to its nominal composition.
4. The sample prepared at larger cooling rate is characterized by better soft magnetic properties.

REFERENCES

[1] R. Hasegawa, Soft magnetic properties of metallic glasses, J. Magn. Magn. Mater. **41**, 79-85 (1984).

[2] J. Zbroszczyk, J. Olszewski, W. Ciurzyńska, B. Wysłocki, R. Kolano, A. Młyńczyk, M. Łukiewski, A. Kolano, J. Lelątko, Microstructure and some magnetic characteristics of amorphous and nanocrystalline $Fe_{83-x}Co_xNb_3B_{13}Cu_1$(x = 0 or 41.5) alloys, J. Magn. Magn. Mater. **254**, 513-515 (2003).

[3] P. Pawlik, M. Nabiałek, E. Żak, J. Zbroszczyk, J. J. Wysłocki, J. Olszewski, K. Pawlik, Processing of bulk amorphous alloys by suction-casting method, Archiwum Nauki o Materiałach **25**, (3), 177-184 (2004).

[4] J. Zbroszczyk, J. Olszewski, W. Ciurzyńska, M. Nabiałek, P. Pawlik, M. Hasiak, A. Łukiewska, K. Perduta, Glass-forming ability and magnetic properties of bulk $Fe_{61}Co_{10}Zr_{2.5}Hf_{2.5}W_2Y_2B_{20}$ (y = 0 or 2, Me = Mo, nB, Ti) alloys, J. Magn. Magn. Mater. **304**, 724-726 (2006).

[5] R. A. Brand, Improving the validity of hyperfine field distributions for magnetic alloys, Nucl. Instrum. Methods, Phys Res **B 28**, 398-416 (1987).

[6] Q. J. Chen, H. B. Fan, J. Shen, J. F. Sun, Z. P. Lu, Critical cooling rate and thermal stability of Fe-Co-Zr-Y-Cr- Mo-B amorphous alloy, J. Alloys and Compounds **407**, 125-128 (2006).

[7] Z. P. Lu, C. T. Liu, A new glass-forming ability criterion for bulk metallic glasses, Acta. Mater. **50**, 3501-3512 (2002).

[8] D. Turnbull, Under what condition can a glass be formed?, Contemp. Phys. **10(5)**, 473-488 (1969).

[9] N. Mitrović, S. Roth, M. Stoica, Magnetic softening of bulk amorphous FeCrMoGaPCB rods by current annealing technique, J. Alloys and Compounds **434-435**, 618-622 (2007).

[10] Q. Chen, D. Zhang, J. Shen, H. Fan, J. Sun, Effect of yttrium on the glass-forming ability of Fe-Cr-Mo-C-B bulk amorphous alloys, J. Alloys and Compounds **27**, 190-193 (2007).

[11] L. Q. Xing, D. M. Herlach, M. Cornet, C. Bertrand, J. P. Dallas, M. F. Trichet, J. P. Chevalier, Mechanical properties of $Zr_{57}Ti_5Al_{10}Cu_{20}Ni_8$ amorphous and partially nanocrystallized alloys, Materials Science and Engineering **A226**, 874-877 (1997).

Received: 10 September 2009.